# Simple DFT scheme for estimating negative electron affinities

Christopher P. Vibert and David J. Tozer*

*Department of Chemistry, Durham University, South Road, Durham, DH1 3LE UK*

E-mail: d.j.tozer@durham.ac.uk

**Abstract**

A simple density functional theory (DFT) scheme is proposed for estimating negative vertical electron affinities of neutral systems, based on a consideration of the integer discontinuity and density scaling homogeneity. The key feature is the derivation of two system-dependent exchange-correlation functionals, one appropriate for the electron deficient side of the integer and one appropriate for the electron abundant side. The electron affinity is evaluated as a linear combination of frontier orbital energies from self-consistent Kohn-Sham calculations on the neutral system using these functionals. For two assessments comprising a total of 43 molecules, the scheme provides electron affinities that are in good agreement with experimental values and which are an improvement over those from the DFT method of Tozer and De Proft [J. Phys. Chem. A **109** 8923 (2005)]. The scheme is trivial to implement in any Kohn-Sham program and the computational cost is that of a series of generalised gradient approximation Kohn-Sham calculations. More generally, the study provides a prescription for performing low-cost, self-consistent Kohn-Sham calculations that yield frontier orbital energies that approximately satisfy the appropriate Koopmans conditions, without the need for exact exchange.

# 1 Introduction and background

The vertical electron affinity of a neutral, $N$-electron system is given by

$$A = E_N - E_{N+1} \tag{1}$$

where $E_N$ and $E_{N+1}$ are the electronic energies of the neutral and anion, respectively, evaluated at the geometry of the neutral. For brevity, we shall omit the term 'vertical' hereafter, but all occurrences of electron affinities (and ionisation potentials) refer to vertical values. Many molecules have negative experimental electron affinities, as measured by electron transmission spectroscopy.[1,2] A negative affinity implies that the anion has an energy above that of the neutral and so is unstable with respect to electron loss. Such anions are short-lived and are termed temporary anions or shape resonances and they play key roles in many areas of science.[3,4] The use of eq (1) with any variational electronic structure method is fundamentally unable to estimate negative affinities − although a negative affinity can be obtained by using compact basis sets, the affinity will approach the variational value of zero as the basis set becomes increasingly diffuse because the description of the anion approaches the neutral plus free electron (assuming no dipole-bound state). Alternative schemes must be used.[3–39]

Tozer and De Proft[22] suggested that negative electron affinities can be estimated in Kohn-Sham density functional theory (DFT)[40] using

$$A = -\left(\epsilon_{\mathrm{LUMO}}^{\mathrm{GGA}} + \epsilon_{\mathrm{HOMO}}^{\mathrm{GGA}} + I^{\mathrm{GGA}}\right) \tag{2}$$

where $\epsilon_{\mathrm{LUMO}}^{\mathrm{GGA}}$ and $\epsilon_{\mathrm{HOMO}}^{\mathrm{GGA}}$ are the lowest unoccupied molecular orbital (LUMO) and highest occupied molecular orbital (HOMO) energies of the neutral, from calculations using a generalised gradient approximation (GGA) exchange-correlation functional. The quantity $I^{\mathrm{GGA}}$ is the corresponding ionisation potential, obtained as the difference between neutral and cation GGA energies, in analogy to eq (1). Their method has been applied successfully,[24–28,30] but

there remains scope for quantitative improvement, particularly for systems where the magnitude of the negative affinity is large. Very recently, Zhang *et al.*[39] applied a DFT global scaling correction method to the calculation of negative affinities, yielding accuracy that surpasses that of eq (2) for modest magnitude affinities.

Central to the methods of Tozer and De Proft and Zhang *et al.* − and also to the scheme proposed in the present study − is the integer discontinuity analysis of Perdew, Parr, Levy, and Balduz.[41] These authors demonstrated that the variation in exact electronic energy as a function of electron number is piecewise linear, meaning that the exact exchange-correlation potential jumps discontinuously as the electron number increases through integer. For a given integer, the exact potential in the limit that the electron number approaches the integer from below (hereafter termed 'electron deficient') is denoted $v_{\rm xc}^{-}(\mathbf{r})$. This potential vanishes asymptotically ($r \rightarrow \infty$) and can be routinely estimated from correlated *ab initio* densities using methods such as that of Zhao-Morrison-Parr (ZMP)[42] or Wu-Yang (WY)[43]/Lieb.[44] A Kohn-Sham calculation on the neutral using the exact $v_{\rm xc}^{-}(\mathbf{r})$ yields a HOMO energy that satisfies the exact Koopmans condition

$$\epsilon_{\rm HOMO}^{-} = -I \tag{3}$$

where $I$ is the exact ionisation potential.[45–47]

We can also define an exact potential in the limit that the electron number approaches the integer from above (hereafter termed 'electron abundant'). This potential, denoted $v_{\rm xc}^{+}(\mathbf{r})$, is shifted from $v_{\rm xc}^{-}(\mathbf{r})$ by the discontinuity constant[41,48,49]

$$v_{\rm xc}^{+}(\mathbf{r}) = v_{\rm xc}^{-}(\mathbf{r}) + \Delta_{\rm xc}\,. \tag{4}$$

Strictly speaking, for finite systems eq (4) holds everywhere except at infinity, where $v_{\rm xc}^{+}(\mathbf{r})$ reduces to zero[46,47] but this is of no consequence in practical calculations. A Kohn-Sham calculation on the neutral using the exact $v_{\rm xc}^{+}(\mathbf{r})$ yields a LUMO energy that satisfies the

exact Koopmans condition

$$\epsilon^{+}_{\mathrm{LUMO}} = -A \tag{5}$$

where $A$ is the exact electron affinity in eq (1).[45–47] It follows from Eqs (4) and (5) that the LUMO energy obtained from a calculation using $v^{-}_{\mathrm{xc}}(\mathbf{r})$ is

$$\epsilon^{-}_{\mathrm{LUMO}} = -A - \Delta_{\mathrm{xc}} \tag{6}$$

and so from Eqs (3) and (6)[46]

$$\Delta_{\mathrm{xc}} = I - A - (\epsilon^{-}_{\mathrm{LUMO}} - \epsilon^{-}_{\mathrm{HOMO}})\,. \tag{7}$$

Another key concept that is central to the present study is that of density scaling homogeneity.[42,50–59] In ref 53, we investigated the density scaling properties of the exact exchange-correlation functional, paying particular attention to the influence of the integer discontinuity. We quantified the behaviour using a homogeneity parameter[42]

$$k_{\mathrm{xc}} = \frac{\int v_{\mathrm{xc}}(\mathbf{r})\rho(\mathbf{r})\,d\mathbf{r}}{E_{\mathrm{xc}}}, \tag{8}$$

where $E_{\mathrm{XC}}$ is the exchange-correlation energy and $\rho(\mathbf{r})$ is the electron density. The degree of system-dependence of this parameter provides a measure of the degree to which the exact functional is homogeneous under density scaling. (A functional $F[\rho]$ is homogeneous of degree $k$ under density scaling[50] if it satisfies $F[\lambda\rho] = \lambda^k F[\rho]$).

For a series of neutral atoms and small molecules, we used WY/Lieb quantities determined from correlated *ab initio* densities, together with experimental $I$ and $A$ values, to determine near-exact estimates for $v^{-}_{\mathrm{xc}}(\mathbf{r})$, $v^{+}_{\mathrm{xc}}(\mathbf{r})$ (using Eqs (4) and (7)), and the average of the two, denoted $v^{\mathrm{av}}_{\mathrm{xc}}(\mathbf{r})$. These quantities, together with the correlated densities and

near-exact estimates for $E_{\rm xc}$, were used to determine near-exact homogeneity parameters associated with the three potentials, namely

$$k_{\rm xc}^{-} = \frac{\int v_{\rm xc}^{-}(\mathbf{r})\rho(\mathbf{r})\,d\mathbf{r}}{E_{\rm xc}}\,, \tag{9}$$

$$k_{\rm xc}^{+} = \frac{\int v_{\rm xc}^{+}(\mathbf{r})\rho(\mathbf{r})\,d\mathbf{r}}{E_{\rm xc}} = k_{\rm xc}^{-} + \frac{N\Delta_{\rm xc}}{E_{\rm xc}}\,, \tag{10}$$

and

$$k_{\rm xc}^{\rm av} = \frac{\int v_{\rm xc}^{\rm av}(\mathbf{r})\rho(\mathbf{r})\,d\mathbf{r}}{E_{\rm xc}} = k_{\rm xc}^{-} + \frac{N\Delta_{\rm xc}}{2E_{\rm xc}}\,, \tag{11}$$

where $N$ is the electron number. We observed[53] that whereas $k_{\rm xc}^{-}$ and $k_{\rm xc}^{+}$ were relatively system-dependent, the value of $k_{\rm xc}^{\rm av}$ was relatively system-independent and close to 4/3. Of particular relevance to the present study was the nature of the electron affinity used in eq (7). For systems with positive experimental affinities there is no choice to make and the $k_{\rm xc}^{\rm av} \approx 4/3$ observation was made. For systems with negative experimental affinities, however, one could choose to use either the negative value or the variational value of zero. *The $k_{xc}^{av} \approx 4/3$ observation was only made when the negative affinity was used.* It follows that for systems with negative experimental affinities, any reasonable exchange-correlation functional that is approximately homogeneous of degree 4/3 yields a potential that approximately averages over the discontinuity computed using the negative affinity (eq (7)). This is consistent with the observation we made in ref 60 that local functionals such as GGAs yield potentials that approximately average in the same way − such functionals are dominated by Dirac exchange and so are, by definition, approximately homogeneous of degree 4/3. Ref 60 also provides insight into the non-ground state nature of the anions when the affinities are negative, through an energy vs. electron number perspective.

In subsequent work, Gledhill and Tozer (GT)[58] showed that the $k_{\rm xc}^{\rm av} \approx 4/3$ observation could be exploited − in conjunction with the known behaviour[60] of GGA functionals regarding the integer discontinuity − to determine a system-dependent exchange-correlation

functional appropriate for the electron deficient side of the integer, i.e. a functional whose potential resembles $v_{\rm xc}^{-}(\mathbf{r})$. This was achieved by demanding that the homogeneity parameter in eq (8) approximately equals the exact $k_{\rm xc}^{-}$ in eq (9). The scheme uses only GGA information to estimate the exact $k_{\rm xc}^{-}$, but it works well, yielding HOMO energies that approximately equal the negative of the ionisation potential (as required, see eq (3)). See ref 58 and Section 2 for further details.

In light of this, it is natural to ask whether an analogous GT approach based on the $k_{\rm xc}^{\rm av} \approx 4/3$ observation could be used to determine an exchange-correlation functional appropriate for the electron abundant side, for which the LUMO energies would approximately equal the negative of the electron affinity (as required, see eq (5)). If so, then this would provide a scheme for estimating the electron affinity as the negative of a LUMO energy. And following the discussion above, the affinity obtained would be an estimate for the negative value, as desired, in cases where the experimental value is negative.

The aim of the present study is to investigate the use of the GT approach for estimating negative electron affinities. The methodology is presented in Section 2. Results and conclusions are presented in Sections 3 and 4, respectively.

# 2 Methodology

The obvious way forward is to use the GT approach to derive an exchange-correlation functional appropriate for the electron abundant side of the integer and estimate the electron affinity as the negative of its LUMO energy. There is, however, an immediate problem.

In ref 58, GT determined a functional appropriate for the electron deficient side of the integer, so required a potential with a $-1/r$ asymptotic form; this was easily achieved by including a Fermi-Amaldi[61] component in their functional. We instead wish to determine a functional appropriate for the electron abundant side of the integer, for which the asymptotic potential is $-1/r + \Delta_{\rm xc}$ (from eq (4)). Writing down a functional form whose potential

recovers the discontinuity constant $\Delta_{\mathrm{xc}}$ is a major challenge. For the present study, we limit ourselves (as is usually[62] the case) to functionals with asymptotically vanishing potentials, which means we face a fundamental problem: such potentials cannot support positive LUMO energies. (Positive values can be obtained, but they will approach zero, indicating unbound orbitals, as the basis set becomes increasingly diffuse[63]). But our aim is to compute a LUMO energy that is the negative of a negative electron affinity, i.e. a positive value! So this is a non-starter.

We therefore instead consider an *indirect* GT approach for estimating the LUMO energy on the electron abundant side. The basic idea is to identify negative LUMO energies (i.e. ones that do not suffer from the aforementioned problem) and then adjust these to make them appropriate for the electron abundant side, through a consideration of the integer discontinuity. There are many ways to achieve this. We now briefly summarise the approaches we considered and identify an optimal scheme. Full methodological details are then presented for that optimal scheme.

First we need to identify functionals that yield negative LUMO energies. An obvious choice is the original electron deficient functional proposed by GT in ref 58. We also consider a second electron deficient functional, obtained by using the same approach, but without the Fermi-Amaldi component in the functional. Given the central role of 4/3 homogeneity, we also use the GT approach to derive a functional whose homogeneity parameter is exactly 4/3 (essentially a GGA-type functional), whose potential approximately averages over the discontinuity; the omission of Fermi-Amaldi is essential in this case since the lack of a discontinuity constant would lead to distortion in the shape of the potential if it was included. For the systems considered (see later), all three functionals yield negative LUMO energies, as required.

Next, we need to adjust these LUMO energies to make them appropriate for the electron abundant side. In the exact case, the electron abundant exchange-correlation potential is simply shifted from the average and electron deficient potentials, meaning the orbital energies

are shifted in the same way. It follows that we must add $\Delta_{xc}$ to the LUMO energy from the two electron deficient functionals and we must add $\Delta_{xc}/2$ to the LUMO energy from the 4/3 functional. We therefore need an estimate for $\Delta_{xc}$ and we obtain this by again exploiting the fact that it does nothing more than shift the orbital energies: providing we have a reliable orbital energy from two different functionals then $\Delta_{xc}$ can be estimated in terms of its difference. Specifically, $\Delta_{xc}$ can be estimated as twice the difference between a given orbital energy from the average 4/3 functional and the same orbital energy from either of the electron deficient functionals. For the systems considered, all three functionals yield negative HOMO energies so we choose to use the differences of HOMO energies, although other orbitals with negative energies could be used. In addition to these two approximations for $\Delta_{xc}$, we also return to the idea of an electron abundant functional, applying the GT procedure to the electron abundant side, for which the HOMO energy (unlike the LUMO) is actually negative for the systems considered. Again, we omit the Fermi-Amaldi component to avoid distortion of the potential. This provides three additional estimates for $\Delta_{xc}$: twice the difference between the HOMO energy of this electron abundant functional and the HOMO energy of the average 4/3 functional; together with the difference between the HOMO energy of this electron abundant functional and the HOMO energy of either of the electron deficient functionals. So we have a total of five estimates for $\Delta_{xc}$, which can be combined with the three estimates for the LUMO energy, yielding 15 estimates for the LUMO energy on the electron abundant side. The negative of this LUMO energy defines the electron affinity. We computed affinities for the 14 systems in ref 22 (see later for details) using the 15 schemes and identified the optimal scheme as the one with the smallest mean absolute error relative to the experimental affinities. The smallest mean absolute error was 0.55 eV; the next smallest was 0.69 eV and the largest was 2.62 eV.

The optimal scheme is to use the LUMO energy from the electron deficient functional (no Fermi-Amaldi), and to shift it by the value of $\Delta_{xc}$, estimated as the difference between the HOMO energies from the electron abundant and electron deficient functionals (again, both

without Fermi-Amaldi). The scheme has a pleasing simplicity, with consistency between electron deficient/abundant functional forms. The full methodological details of the scheme are now described; for additional details of the GT approach that underlies the scheme, see ref 58.

1. For the neutral system whose electron affinity is to be computed, a GGA calculation is first performed, yielding the exchange-correlation energy, $E_{\rm xc}^{\rm GGA}$, and HOMO energy, $\epsilon_{\rm HOMO}^{\rm GGA}$. A GGA calculation is also performed on the cation and the neutral/cation energies are used to compute the ionisation potential, $I^{\rm GGA}$.

2. Two new *system-dependent* exchange-correlation functionals then need to be derived. They each have the mathematical form,

$$E_{\rm xc}^{\pm} = \alpha^{\pm} G_{\rm xc}^{\pm} \,, \tag{12}$$

where the $\pm$ superscript indicates either the electron deficient ($-$) or electron abundant ($+$) functional. Here, $\alpha^{\pm}$ are parameters and

$$G_{\rm xc}^{\pm} = \left[ \int \rho^{\frac{3k^{\pm}}{3k^{\pm}-1}}(\mathbf{r}) d\mathbf{r} \right]^{\frac{3k^{\pm}-1}{3}} \tag{13}$$

are local functionals of the form considered by Liu and Parr,[51] which are homogeneous of degree $k^{\pm}$ under density scaling (meaning that the evaluation of eq (8) for the functional in eq (12) yields $k_{\rm xc} = k^{\pm}$). They are homogenous of degree 1 under the more common coordinate scaling.[64] The values of $\alpha^{\pm}$ and $k^{\pm}$ are to be determined on a system-by-system basis.

3. For the electron deficient functional, the value of the homogeneity parameter $k^{-}$ must approximate the exact $k_{\rm xc}^{-}$ in eq (9), which can be expressed alternatively as

$$k_{\rm xc}^{-} = k_{\rm xc}^{\rm av} - \frac{N\Delta_{\rm xc}}{2E_{\rm XC}} \,, \tag{14}$$

through rearrangement of eq (11). We know that $k_{\rm xc}^{\rm av} \approx 4/3$ and, following refs 58,60, we approximate $\Delta_{\rm xc}$ as

$$\Delta_{\rm xc} \approx 2(\epsilon_{\rm HOMO}^{\rm GGA} + I^{\rm GGA}) \tag{15}$$

(which reflects the fact that a GGA functional approximately averages over the discontinuity computed using the negative $A$; see earlier discussion). We also approximate the exchange-correlation energy by the GGA value. Using these approximations in eq (14) yields the value of $k^-$ to be used in eq (13),

$$k^- = \frac{4}{3} - \frac{N(\epsilon_{\rm HOMO}^{\rm GGA} + I^{\rm GGA})}{E_{\rm xc}^{\rm GGA}}\,, \tag{16}$$

which is evaluated using the quantities from the prior GGA calculations. This is a simplified version of eq (19) of ref 58, reflecting the absence of Fermi-Amaldi in the present study.

4. The value of $k^+$ must approximate the exact $k_{\rm xc}^+$ in eq (10). By analogy with $k^-$ we have

$$\begin{aligned} k^+ &= \frac{4}{3} + \frac{N(\epsilon_{\rm HOMO}^{\rm GGA} + I^{\rm GGA})}{E_{\rm xc}^{\rm GGA}} \\ &= \frac{8}{3} - k^-\,, \end{aligned} \tag{17}$$

where $k^-$ is given in eq (16).

5. The values of $\alpha^\pm$ are then obtained from the requirement that the evaluation of the exchange-correlation energy of the neutral using the GGA density yields the GGA exchange-correlation energy. From eq (12), this simply requires

$$\alpha^\pm = \frac{E_{\rm xc}^{\rm GGA}}{G_{\rm xc}^{\pm,{\rm GGA}}} \tag{18}$$

where $G_{\rm xc}^{\pm,{\rm GGA}}$ is obtained by evaluating $G_{\rm xc}^\pm$ in eq (13) using the GGA density for the neutral, using the above values of $k^\pm$.

6. Having established the values of the parameters $k^{\pm}$ and $\alpha^{\pm}$, standard self-consistent Kohn-Sham calculations are performed on the neutral using the electron deficient functional, $E_{\rm xc}^{-}$, and electron abundant functional, $E_{\rm xc}^{+}$. For the implementation of the exchange-correlation potential, the functional derivative of the functional in eq (13) is given in eq (23) of ref 59. The LUMO energy on the electron abundant side is then estimated as

$$\epsilon_{\rm LUMO}^{+,{\rm est}} = \epsilon_{\rm LUMO}^{-} + \epsilon_{\rm HOMO}^{+} - \epsilon_{\rm HOMO}^{-} \tag{19}$$

where $\epsilon_{\rm LUMO}^{-}$ and $\epsilon_{\rm HOMO}^{-}$ are the LUMO and HOMO energies obtained from calculations using the electron deficient functional and $\epsilon_{\rm HOMO}^{+}$ is the HOMO energy obtained from calculations using the electron abundant functional. As noted above, this should be interpreted as the LUMO energy on the electron deficient side, shifted by the discontinuity constant, estimated as the difference between the HOMO energies from the electron abundant and electron deficient functionals. Finally, the electron affinity is defined to be the negative of this LUMO energy,

$$\begin{aligned} A &= -\epsilon_{\rm LUMO}^{+,{\rm est}} \\ &= -\left(\epsilon_{\rm LUMO}^{-} + \epsilon_{\rm HOMO}^{+} - \epsilon_{\rm HOMO}^{-}\right) . \end{aligned} \tag{20}$$

It is pertinent to compare eq (20) with the Tozer-De Proft expression in eq (2). In the latter, the electron affinity can again be interpreted as the negative of a LUMO energy on the electron abundant side. However, the LUMO energy is estimated as the LUMO energy of a near-average GGA functional, shifted by half the discontinuity constant estimated using Eq (15); it is a pure GGA method with no involvement of density scaling.

Both the scheme proposed here and the Tozer-De Proft method require GGA Kohn-Sham calculations on the neutral and cation. The former requires three further Kohn-Sham calculations on the neutral, one to evaluate $G_{\rm xc}^{\pm,{\rm GGA}}$ in eq (18) and two self-consistent calculations using $E_{\rm xc}^{\pm}$; none of these are more costly than a GGA calculation.

In Section 3, we compare electron affinities determined using Eqs (2) and (20). For the GGA, we use the Perdew-Burke-Ernzerhof (PBE) functional[65] throughout. All calculations are performed using the aug-cc-pVTZ basis set with the CADPAC[66] program.

# 3 Results

We start by considering the 14 small molecules considered previously in ref 22, namely $F_2$, $Cl_2$, $H_2CO$, $C_2H_4$, CO, $PH_3$, $H_2S$, HCN, HCl, $CO_2$, $NH_3$, HF, $H_2O$, and $CH_4$. The first two molecules actually have positive experimental electron affinities, whereas the remainder are negative, becoming increasingly so across the series. Although the focus of the new methodology is on the calculation of negative affinities, the scheme is equally applicable to positive affinities; in practice, of course, eq (1) is unproblematic in such cases. Calculations are performed at the near-experimental geometries of refs 22,67 and the affinities are compared with the experimental values of ref 22.

To fully illustrate the scheme, Table 1 lists the parameters that define $E_{\rm xc}^-$ and $E_{\rm xc}^+$, together with the HOMO and LUMO energies obtained from self-consistent calculations using those functionals. Also listed are the values of $\epsilon_{\rm LUMO}^{+,\rm est}$, determined using eq (19). The impracticability of using the directly computed $\epsilon_{\rm LUMO}^+$ is clearly evident: for all the systems with negative experimental electron affinities, the values of $\epsilon_{\rm LUMO}^+$ are marginally positive, but given that the potential vanishes asymptotically, it follows that these values will all approach zero as the basis set becomes increasingly diffuse.[63] By contrast, the values of $\epsilon_{\rm LUMO}^{+,\rm est}$ are significantly more positive and − given that all the orbital energies that contribute to this quantity through eq (19) are negative − it follows that the values of $\epsilon_{\rm LUMO}^{+,\rm est}$ will change only marginally as the basis set becomes increasingly diffuse.

Table 2 presents the electron affinities determined using eq (2), together with affinities determined using the new expression, Eq (20) (i.e. the negative of the $\epsilon_{\rm LUMO}^{+,\rm est}$ values in Table 1, converted into eV). Experimental affinities are also presented, together with mean

Table 1: Functional parameters defining $E_{\rm xc}^{-}$ and $E_{\rm xc}^{+}$, together with their associated orbital energies and the estimated LUMO energy in eq (19). All values are in a.u.

| | $k^-$ | $\alpha^-$ | $\epsilon^-_{\rm HOMO}$ | $\epsilon^-_{\rm LUMO}$ | $k^+$ | $\alpha^+$ | $\epsilon^+_{\rm HOMO}$ | $\epsilon^+_{\rm LUMO}$ | $\epsilon^{+,\rm est}_{\rm LUMO}$ |
|---|---|---|---|---|---|---|---|---|---|
| $F_2$ | 1.523 | −0.509 | −0.554 | −0.424 | 1.144 | −1.338 | −0.183 | −0.061 | −0.053 |
| $Cl_2$ | 1.420 | −0.622 | −0.345 | −0.232 | 1.247 | −1.061 | −0.180 | −0.074 | −0.068 |
| $H_2CO$ | 1.515 | −0.539 | −0.378 | −0.239 | 1.152 | −1.293 | −0.101 | +0.011 | +0.037 |
| $C_2H_4$ | 1.521 | −0.536 | −0.376 | −0.161 | 1.145 | −1.324 | −0.139 | +0.021 | +0.076 |
| CO | 1.514 | −0.553 | −0.481 | −0.223 | 1.153 | −1.260 | −0.205 | +0.035 | +0.054 |
| $PH_3$ | 1.437 | −0.637 | −0.321 | −0.065 | 1.229 | −1.049 | −0.159 | +0.007 | +0.097 |
| $H_2S$ | 1.437 | −0.635 | −0.309 | −0.081 | 1.230 | −1.046 | −0.143 | +0.004 | +0.086 |
| HCN | 1.536 | −0.528 | −0.494 | −0.190 | 1.131 | −1.325 | −0.199 | +0.017 | +0.106 |
| HCl | 1.442 | −0.623 | −0.389 | −0.096 | 1.224 | −1.058 | −0.194 | +0.005 | +0.099 |
| $CO_2$ | 1.499 | −0.528 | −0.491 | −0.166 | 1.168 | −1.316 | −0.206 | +0.020 | +0.118 |
| $NH_3$ | 1.554 | −0.546 | −0.384 | −0.086 | 1.112 | −1.272 | −0.095 | +0.016 | +0.202 |
| HF | 1.562 | −0.527 | −0.574 | −0.126 | 1.104 | −1.278 | −0.180 | +0.018 | +0.268 |
| $H_2O$ | 1.554 | −0.542 | −0.447 | −0.107 | 1.112 | −1.263 | −0.120 | +0.015 | +0.221 |
| $CH_4$ | 1.576 | −0.525 | −0.512 | −0.066 | 1.091 | −1.335 | −0.200 | +0.021 | +0.247 |

Table 2: Electron affinities (in eV).

| | eq (2) | eq (20) | Expt |
|---|---|---|---|
| $F_2$ | −0.10 | +1.44 | +1.24 |
| $Cl_2$ | +0.34 | +1.84 | +1.02 |
| $H_2CO$ | −1.84 | −1.01 | −1.5 |
| $C_2H_4$ | −2.82 | −2.06 | −1.8 |
| CO | −2.82 | −1.46 | −1.8 |
| $PH_3$ | −3.16 | −2.65 | −1.9 |
| $H_2S$ | −3.24 | −2.33 | −2.1 |
| HCN | −3.81 | −2.88 | −2.3 |
| HCl | −3.58 | −2.71 | −3.3 |
| $CO_2$ | −3.70 | −3.22 | −3.8 |
| $NH_3$ | −4.06 | −5.49 | −5.6 |
| HF | −5.70 | −7.29 | −6.0 |
| $H_2O$ | −4.62 | −6.00 | −6.4 |
| $CH_4$ | −4.15 | −6.71 | −7.8 |
| MAD | 1.14 | 0.55 | |

absolute deviations (MADs) relative to these experimental values. Eq (2) works reasonably well, with a MAD of 1.14 eV; the largest deviations are for systems where the magnitude of the experimental affinity is largest. In moving to eq (20), the MAD is reduced by more than a factor of two to 0.55 eV. The deviations are more uniform, although they can still be in excess of 1 eV and there is no obvious pattern to them; they reflect the approximations underlying the approach. To put the results into context, the MAD when eq (1) is used is 2.8 eV. (See ref 22 for numerical values). Evaluating the affinity as the negative of the directly computed $\epsilon^{+}_{\rm LUMO}$, rather than the negative of $\epsilon^{+,\rm est}_{\rm LUMO}$, yields a similar MAD of 2.9 eV.

Figure 1 presents scatter plots of these calculated vs. experimental electron affinities. The dotted lines indicate perfect agreement; the solid lines are the lines of best fit and the corresponding $R^2$ values are listed. The improvement from eq (2) to eq (20) is pronounced, with $R^2$ increasing from 0.76 to 0.94.

As a second application, we consider the 29 molecules of Table 3, drawn from the studies in refs 24,25, using the same B3LYP/6-311+G** geometries; electron affinities are compared with the experimental values described in these earlier studies. The functional parameters and orbital energies exhibit the same features and signs as those in Table 1 and so we do not present the individual values. Table 3 presents the affinities determined using Eqs (2) and (20), together with experimental values and MADs. The MAD using eq (2) is 0.50 eV. This is a notable improvement over that in Table 2, reflecting the fact that the magnitudes of the experimental affinities are not large for these systems. All 29 affinities are, however, underestimated (too negative). In moving to eq (20), all the affinities increase and the MAD reduces by almost a factor of three, to 0.17 eV. Figure 2 presents scatter plots, where the improvement in absolute accuracy is clearly evident. Both methods yield good $R^2$ values, although the value is marginally better with Eq (20).

Zhang *et al.*[39] also included these 29 molecules (with the same basis set and geometries) in their recent investigation of negative electron affinities from a DFT global scaling method and so we can make a direct comparison between the methods. For the molecules in Table 3

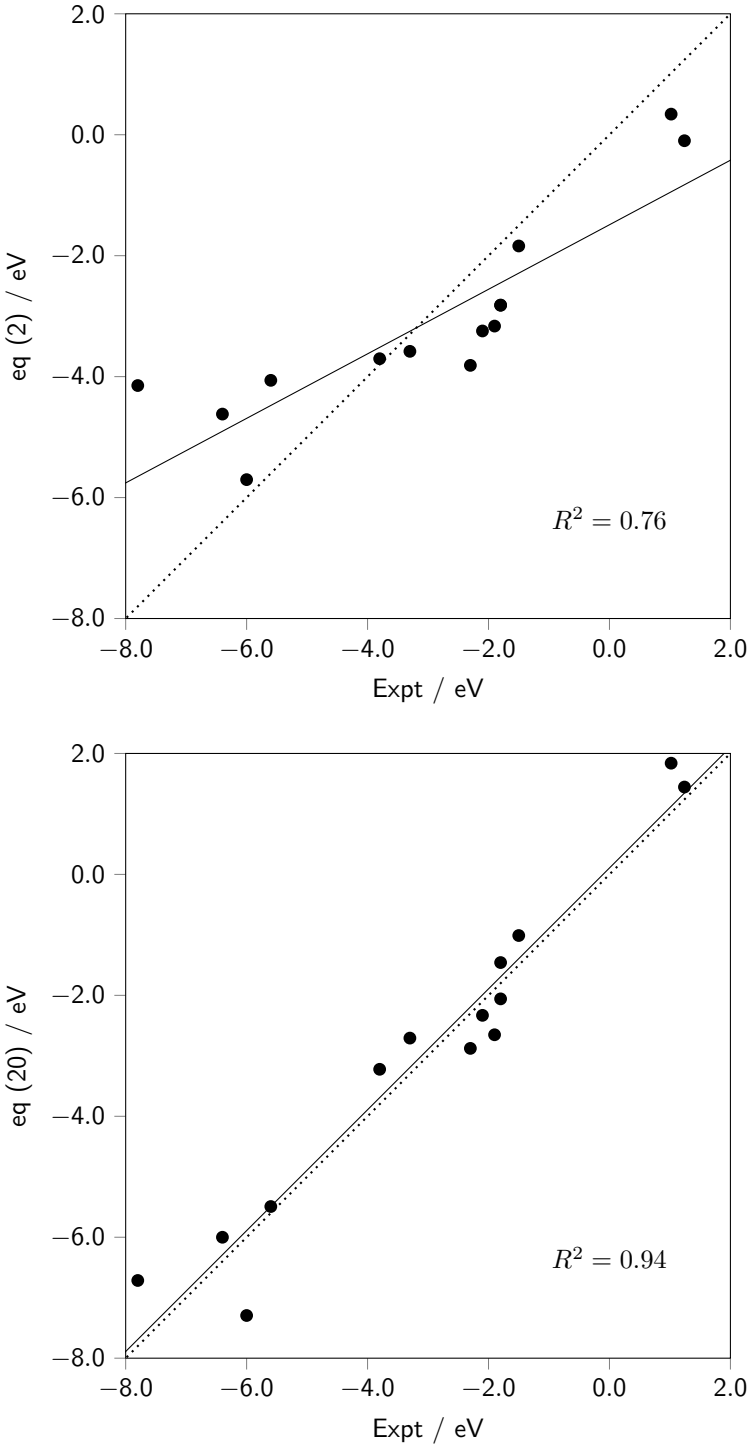


Figure 1: Scatter plots of calculated vs. experimental electron affinities. Data from Table 2.

Table 3: Electron affinities (in eV).

| | eq (2) | eq (20) | Expt |
|---|---|---|---|
| Pyrazine | −0.55 | +0.03 | −0.07 |
| Naphthalene | −0.34 | +0.22 | −0.20 |
| Pyrimidine | −0.88 | −0.24 | −0.25 |
| Styrene | −0.51 | +0.03 | −0.25 |
| Pyridazine | −0.87 | −0.16 | −0.32 |
| Cytosine | −0.84 | −0.18 | −0.36 |
| Tricholoroethylene | −1.02 | −0.11 | −0.58 |
| Guanine | −1.17 | −0.53 | −0.64 |
| Adenine | −0.96 | −0.31 | −0.64 |
| Chlorobenzene | −1.15 | −0.50 | −0.75 |
| 1,3−Cyclohexadiene | −1.14 | −0.56 | −0.80 |
| Trans−dichloroethylene | −1.35 | −0.46 | −0.82 |
| Fluorobenzene | −1.41 | −0.81 | −0.87 |
| Phenol | −1.59 | −1.04 | −1.01 |
| Norbornadiene | −1.54 | −1.04 | −1.04 |
| m−Xylene | −1.57 | −1.10 | −1.06 |
| Anisole | −1.55 | −1.03 | −1.09 |
| Cis−dichloroethylene | −1.52 | −0.55 | −1.12 |
| Aniline | −1.71 | −1.18 | −1.13 |
| Acetaldehyde | −2.04 | −1.21 | −1.19 |
| Acetone | −2.14 | −1.46 | −1.51 |
| Furan | −2.37 | −1.58 | −1.76 |
| Ethylene | −2.82 | −2.07 | −1.78 |
| Propene | −2.74 | −2.17 | −1.99 |
| Cyclohexene | −2.45 | −2.16 | −2.07 |
| Trans−butene | −2.77 | −2.31 | −2.10 |
| Cis−butene | −2.70 | −2.22 | −2.22 |
| Trimethylethylene | −2.51 | −2.22 | −2.24 |
| Pyrrole | −2.50 | −2.26 | −2.38 |
| MAD | 0.50 | 0.17 | |

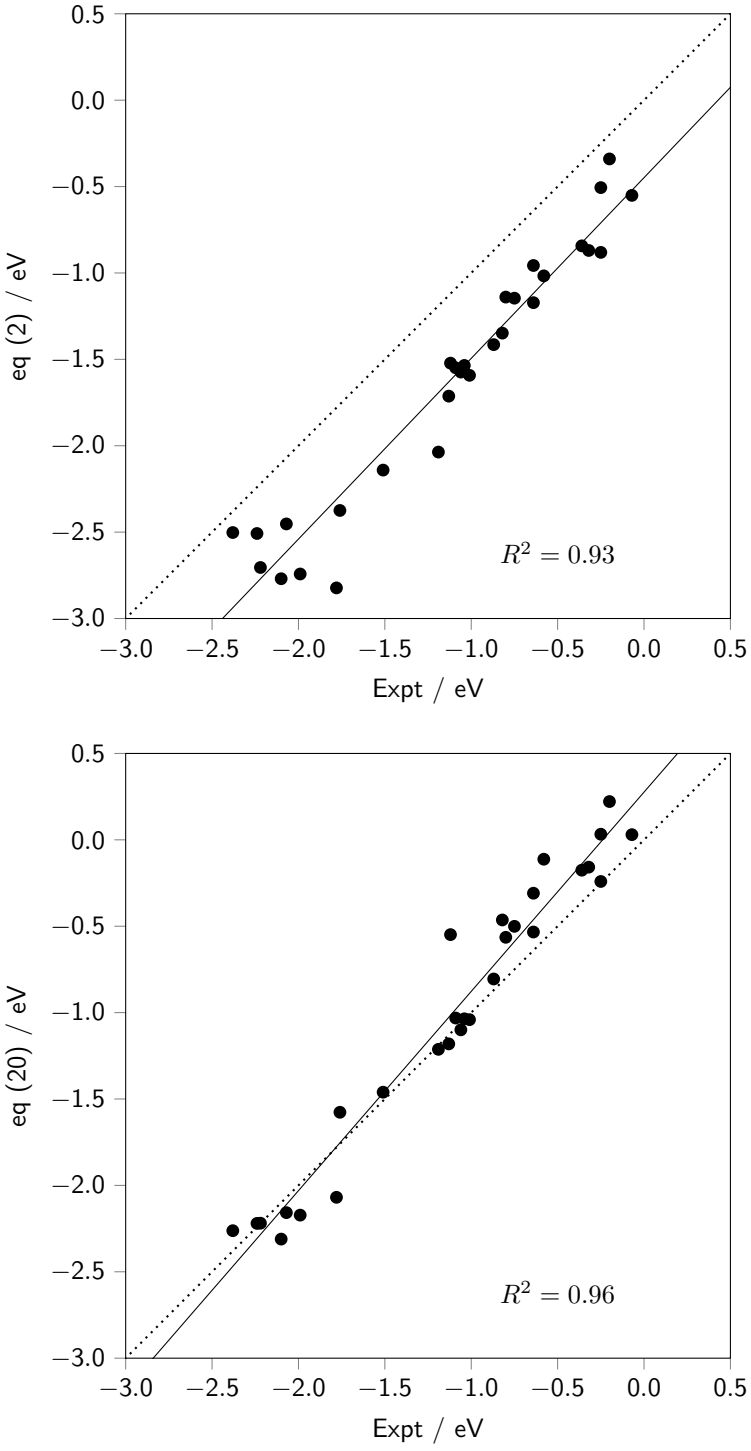


Figure 2: Scatter plots of calculated vs. experimental electron affinities. Data from Table 3.

and Figure 2, the MAD from their method is 0.18 eV and $R^2 = 0.93$, indicating very similar overall performance to eq (20). Zhang *et al* noted that for four of the molecules, they needed to choose the LUMO+1 (rather than LUMO) as the frontier orbital to perform their scaling correction and they attributed this to delocalisation error in the underlying PBE functional. No such correction was necessary in the present study.

# 4 Conclusions

We have proposed a simple DFT scheme for estimating negative electron affinities of neutral systems. The key feature is the derivation of two system-dependent exchange-correlation functionals, one appropriate for the electron deficient side of the integer and one appropriate for the electron abundant side. For the systems considered, the scheme yields affinities that are an improvement over those from the Tozer-De Proft expression. The scheme is trivial to implement in any Kohn-Sham program and the calculations are low cost.

The study can also be viewed from an alternative perspective: It provides a prescription for performing self-consistent Kohn-Sham calculations that yield frontier orbital energies that approximately satisfy the appropriate Koopmans conditions. Specifically, the orbital energy $\epsilon_{\mathrm{LUMO}}^{+,\mathrm{est}}$ in eq (19) approximates the negative of the electron affinity (both negative and positive values; see earlier), whilst the orbital energy $\epsilon_{\mathrm{HOMO}}^{-}$, evaluated from self-consistent calculations using $E_{\mathrm{xc}}^{-}$, approximates the negative of the ionisation potential (as it did in ref 58). For the orbital energies in Table 1, the MAD between $\epsilon_{\mathrm{LUMO}}^{+,\mathrm{est}}$ and the experimental $-A$ values is 0.55 eV (Table 2), whilst the MAD between $\epsilon_{\mathrm{HOMO}}^{-}$ and the experimental $-I$ values from ref 22 is 0.93 eV. These deviations are factors of 8 and 5 times smaller, respectively, than the deviations obtained when GGA orbital energies are used, although the increase in computational cost associated with the improvement is minimal. Notably, there is no exact exchange in the methodology. The ability to perform such calculations − together with the theoretical ideas that underly them − are likely to be useful in other research areas where

orbital energies, ionisation potentials, electron affinities, and the integer discontiniuty play a key role.

# 5 Acknowledgments

We are grateful to Nick Sablon for providing the molecular geometries used in refs 24,25.

# References

(1) Sanche, L.; Schulz, G. J. Electron Transmission Spectroscopy: Rare Gases. *Phys. Rev. A* **1972**, *5*, 1672–1683.

(2) Jordan, K. D.; Burrow, P. D. Temporary anion states of polyatomic hydrocarbons. *Chem. Rev.* **1987**, *87*, 557–588.

(3) Jagau, T.-C.; Bravaya, K. B.; Krylov, A. I. Extending Quantum Chemistry of Bound States to Electronic Resonances. *Ann. Rev. Phys. Chem.* **2017**, *68*, 525–553.

(4) Simons, J. Theoretical Study of Negative Molecular Ions. *Annual Review of Physical Chemistry* **2011**, *62*, 107–128.

(5) Hazi, A. U.; Taylor, H. S. Stabilization Method of Calculating Resonance Energies: Model Problem. *Phys. Rev. A* **1970**, *1*, 1109–1120.

(6) Taylor, H. S.; Hazi, A. U. Comment on the stabilization method: Variational calculation of the resonance width. *Phys. Rev. A* **1976**, *14*, 2071–2074.

(7) Simons, J. Resonance state lifetimes from stabilization graphs. *J. Chem. Phys.* **1981**, *75*, 2465–2467.

(8) Frey, R. F.; Simons, J. Resonance state energies and lifetimes via analytic continuation of stabilization graphs. *J. Chem. Phys.* **1986**, *84*, 4462–4469.

(9) Chen, D.; Gallup, G. A. The relationship of the virtual orbitals of self-consistent-field theory to temporary negative ions in electron scattering from molecules. *J. Chem. Phys.* **1990**, *93*, 8893–8901.

(10) Guerra, M. On the use of diffuse functions for estimating negative electron affinities with LCAO methods. *Chem. Phys. Lett.* **1990**, *167*, 315–319.

(11) Riss, U. V.; Meyer, H. D. Calculation of resonance energies and widths using the complex absorbing potential method. *J. Phys. B* **1993**, *26*, 4503.

(12) Chen, C.-S.; Feng, T.-H.; Chao, J. S.-Y. Stabilized Koopmans' Theorem Calculations on the $\pi^*$ Temporary Anion States of Benzene and Substituted Benzenes. *J. Phys. Chem.* **1995**, *99*, 8629–8632.

(13) Sommerfeld, T.; Cederbaum, L. S. Long-Lived States of $N_2^-$. *Phys. Rev. Lett.* **1998**, *80*, 3723–3726.

(14) Szarka, A. Z.; Curtiss, L. A.; Miller, J. R. Calculation of temporary anion states using density functional theory. *Chem. Phys.* **1999**, *246*, 147–155.

(15) Falcetta, M. F.; Jordan, K. D. Ab initio investigation of the temporary anion states of silane and the linear silanes: $(Si_nH_{2n+2})$, $n = 2 - 5$. *Chem. Phys. Lett.* **1999**, *300*, 588–594.

(16) Falcetta, M. F.; Choi, Y.; Jordan, K. D. Ab Initio Investigation of the Temporary Anion States of Perfluoroethane. *J. Phys. Chem. A* **2000**, *104*, 9605–9612.

(17) Aflatooni, K.; Hitt, B.; Gallup, G. A.; Burrow, P. D. Temporary anion states of selected amino acids. *J. Chem. Phys.* **2001**, *115*, 6489–6494.

(18) Whitehead, A.; Barrios, R.; Simons, J. Stabilization Calculation of the Energy and Lifetime of Metastable $SO_4{}^{2-}$. *J. Chem. Phys.* **2002**, *116*, 2848–2851.

(19) Li, X.; Cai, Z.; Sevilla, M. D. DFT Calculations of the Electron Affinities of Nucleic Acid Bases: Dealing with Negative Electron Affinities. *J. Phys. Chem. A* **2002**, *106*, 1596–1603.

(20) Feuerbacher, S.; Sommerfeld, T.; Santra, R.; Cederbaum, L. S. Complex absorbing potentials in the framework of electron propagator theory. II. Application to temporary anions. *J. Chem. Phys.* **2003**, *118*, 6188–6199.

(21) Vera, D. M. A.; Pierini, A. B. Species with negative electron affinity and standard DFT methods. *Phys. Chem. Chem. Phys.* **2004**, *6*, 2899–2903.

(22) Tozer, D. J.; De Proft, F. Computation of the Hardness and the Problem of Negative Electron Affinities in Density Functional Theory. *J. Phys. Chem. A* **2005**, *109*, 8923–8929.

(23) Modelli, A.; Jones, D. Temporary Anion States and Dissociative Electron Attachment in Diphenyl Disulfide. *J. Phys. Chem. A* **2006**, *110*, 10219–10224.

(24) De Proft, F.; Sablon, N.; Tozer, D. J.; Geerlings, P. Calculation of negative electron affinity and aqueous anion hardness using Kohn-Sham HOMO and LUMO energies. *Faraday Discuss.* **2007**, *135*, 151–159.

(25) Sablon, N.; De Proft, F.; Geerlings, P.; Tozer, D. J. On the position of the potential wall in DFT temporary anion calculations. *Phys. Chem. Chem. Phys.* **2007**, *9*, 5880–5884.

(26) Tozer, D. J.; De Proft, F. Modeling temporary anions in density functional theory: Calculation of the Fukui function. *J. Chem. Phys.* **2007**, *127*, 034108.

(27) Ejsing, A. M.; Brøndsted Nielsen, S. Computational study on the negative electron affinities of $NO_2^-.(H_2O)_n$ clusters ($n$=0–30). *J. Chem. Phys.* **2007**, *126*, 154313.

(28) Hajgato, B.; Deleuze, M. S.; Tozer, D. J.; De Proft, F. A benchmark theoretical study of the electron affinities of benzene and linear acenes. *J. Chem. Phys.* **2008**, *129*, 084308.

(29) Puiatti, M.; Vera, D. M. A.; Pierini, A. B. In search for an optimal methodology to calculate the valence electron affinities of temporary anions. *Phys. Chem. Chem. Phys.* **2009**, *11*, 9013–9024.

(30) Peach, M. J. G.; De Proft, F.; Tozer, D. J. Negative Electron Affinities from DFT: Fluorination of Ethylene. *J. Phys. Chem. Lett.* **2010**, *1*, 2826–2831.

(31) Cheng, H.-Y.; Chen, C.-W. Energy and Lifetime of Temporary Anion States of Uracil by Stabilization Method. *J. Phys. Chem. A* **2011**, *115*, 10113–10121.

(32) Sommerfeld, T.; Weber, R. J. Empirical Correlation Methods for Temporary Anions. *J. Phys. Chem. A* **2011**, *115*, 6675–6682.

(33) Whitenack, D. L.; Wasserman, A. Density Functional Resonance Theory of Unbound Electronic Systems. *Phys. Rev. Lett.* **2011**, *107*, 163002.

(34) Sugohara, R. T.; Homem, M. G. P.; Iga, I.; de Souza, G. L. C.; Machado, L. E.; Ferraz, J. R.; dos Santos, A. S.; Brescansin, L. M.; Lucchese, R. R.; Lee, M. T. Cross sections for electron collisions with dimethyl ether. *Phys. Rev. A* **2013**, *88*, 022709.

(35) Bravaya, K. B.; Zuev, D.; Epifanovsky, E.; Krylov, A. I. Complex-scaled equation-of-motion coupled-cluster method with single and double substitutions for autoionizing excited states: Theory, implementation, and examples. *J. Chem. Phys.* **2013**, *138*, 124106.

(36) Jagau, T.-C.; Zuev, D.; Bravaya, K. B.; Epifanovsky, E.; Krylov, A. I. A Fresh Look at Resonances and Complex Absorbing Potentials: Density Matrix-Based Approach. *J. Phys. Chem. Lett.* **2014**, *5*, 310–315.

(37) Zuev, D.; Jagau, T.-C.; Bravaya, K. B.; Epifanovsky, E.; Shao, Y.; Sundstrom, E.; Head-Gordon, M.; Krylov, A. I. Complex absorbing potentials within EOM-CC family of methods: Theory, implementation, and benchmarks. *J. Chem. Phys.* **2014**, *141*, 024102.

(38) Kunitsa, A. A.; Granovsky, A. A.; Bravaya, K. B. CAP-XMCQDPT2 method for molecular electronic resonances. *J. Chem. Phys.* **2017**, *146*, 184107.

(39) Zhang, D.; Yang, X.; Zheng, X.; Yang, W. Accurate density functional prediction of molecular electron affinity with the scaling corrected Kohn–Sham frontier orbital energies. *Mol. Phys.* **2018**, *116*, 927–934.

(40) Kohn, W.; Sham, L. J. Self-Consistent Equations Including Exchange and Correlation Effects. *Phys. Rev.* **1965**, *140*, A1133–A1138.

(41) Perdew, J. P.; Parr, R. G.; Levy, M.; Balduz, J. L. Density-Functional Theory for Fractional Particle Number: Derivative Discontinuities of the Energy. *Phys. Rev.* **1982**, *49*, 1691–1694.

(42) Zhao, Q.; Morrison, R. C.; Parr, R. G. From electron densities to Kohn-Sham kinetic energies, orbital energies, exchange-correlation potentials, and exchange-correlation energies. *Phys. Rev. A* **1994**, *50*, 2138–2142.

(43) Wu, Q.; Yang, W. A direct optimization method for calculating density functionals and exchange–correlation potentials from electron densities. *J. Chem. Phys.* **2003**, *118*, 2498–2509.

(44) Lieb, E. H. Density functionals for coulomb systems. *Int. J. Quantum Chem.* **1983**, *24*, 243–277.

(45) Janak, J. Proof that $\partial E/\partial n_i = \epsilon_i$ in density-functional theory. *Phys. Rev. B* **1978**, *18*, 7165–7168.

(46) Perdew, J. P.; Levy, M. Physical Content of the Exact Kohn-Sham Orbital Energies: Band Gaps and Derivative Discontinuities. *Phys. Rev. Lett.* **1983**, *51*, 1884–1887.

(47) Baerends, E. J. Density functional approximations for orbital energies and total energies of molecules and solids. *J. Chem. Phys.* **2018**, *149*, 054105.

(48) Sagvolden, E.; Perdew, J. Discontinuity of the exchange-correlation potential: Support for assumptions used to find it. *Phys. Rev. A* **2008**, *77*, 12517.

(49) Lein, M.; Kümmel, S. Exact Time-Dependent Exchange-Correlation Potentials for Strong-Field Electron Dynamics. *Phys. Rev. Lett.* **2005**, *94*, 143003.

(50) Liu, S.; Parr, R. G. Expansions of the correlation-energy density functional and its kinetic-energy component. *Phys. Rev. A* **1996**, *53*, 2211–2219.

(51) Liu, S.; Parr, R. G. Expansions of density functionals in terms of homogeneous functionals:Justification and nonlocal representation of the kinetic energy, exchange energy,and classical Coulomb repulsion energy for atoms. *Phys. Rev. A* **1997**, *55*, 1792–1798.

(52) Tozer, D. J. Effective homogeneity of the exchange-correlation energy functional. *Phys. Rev. A* **1998**, *58*, 3524–3527.

(53) Borgoo, A.; Teale, A. M.; Tozer, D. J. Effective homogeneity of the exchange–correlation and non-interacting kinetic energy functionals under density scaling. *J. Chem. Phys.* **2012**, *136*, 034101.

(54) Borgoo, A.; Tozer, D. J. Negative Electron Affinities from DFT: Influence of Asymptotic Exchange-Correlation Potential and Effective Homogeneity under Density Scaling. *J. Phys. Chem. A* **2012**, *116*, 5497–5500.

(55) Borgoo, A.; Tozer, D. J. Density Scaling of Noninteracting Kinetic Energy Functionals. *J. Chem. Theory Comput.* **2013**, *9*, 2250–2255.

(56) Borgoo, A.; Green, J. A.; Tozer, D. J. Molecular Binding in Post-Kohn–Sham Orbital-Free DFT. *J. Chem. Theory Comput.* **2014**, *10*, 5338–5345.

(57) Borgoo, A.; Teale, A. M.; Tozer, D. J. Revisiting the density scaling of the non-interacting kinetic energy. *Phys. Chem. Chem. Phys.* **2014**, *16*, 14578–14583.

(58) Gledhill, J. D.; Tozer, D. J. System-dependent exchange–correlation functional with exact asymptotic potential and $\epsilon_{\mathrm{HOMO}} \approx -I$. *J. Chem. Phys.* **2015**, *143*, 024104.

(59) Sharpe, D. J.; Levy, M.; Tozer, D. J. Approximating the Shifted Hartree-Exchange-Correlation Potential in Direct Energy Kohn–Sham Theory. *J. Chem. Theory Comput.* **2018**, *14*, 684–692.

(60) Teale, A. M.; De Proft, F.; Tozer, D. J. Orbital Energies and Negative Electron Affinities from Density Functional Theory: Insight from the Integer Discontinuity. *J. Chem. Phys.* **2008**, *129*, 044110.

(61) Fermi, E.; Amaldi, E. Le orbite oos degli elementi. *Accad. Ital. Rome* **1934**, *6*, 117–149.

(62) Aschebrock, T.; Armiento, R.; Kümmel, S. Challenges for semilocal density functionals with asymptotically nonvanishing potentials. *Phys. Rev. B* **2017**, *96*, 075140.

(63) Peach, M. J. G.; Teale, A. M.; Helgaker, T.; Tozer, D. J. Fractional Electron Loss in Approximate DFT and Hartree–Fock Theory. *J. Chem. Theory Comput.* **2015**, *11*, 5262–5268.

(64) Levy, M.; Perdew, J. P. Hellmann-Feynman, virial, and scaling requisites for the exact universal density functionals. Shape of the correlation potential and diamagnetic susceptibility for atoms. *Phys. Rev. A* **1985**, *32*, 2010–2021.

(65) Perdew, J. P.; Burke, K.; Ernzerhof, M. Generalized Gradient Approximation Made Simple. *Phys. Rev. Lett.* **1996**, *77*, 3865–3868.

(66) Amos, R. D.; Alberts, I. L.; Andrews, J. S.; Cohen, A. J.; Colwell, S. M.; Handy, N. C.; Jayatilaka, D.; Knowles, P. J.; Kobayashi, R.; Laming, G. J.; Lee, A. M.; Maslen, P. E.; Murray, C. W.; Palmieri, P.; Rice, J. E.; Simandiras, E. D.; Stone, A. J.; Su, M.-D.; Tozer, D. J. CADPAC 6.5, The Cambridge Analytic Derivatives Package. 1998.

(67) Handy, N. C.; Tozer, D. J. The development of new exchange-correlation functionals: 3. *Mol. Phys.* **1998**, *94*, 707–715.

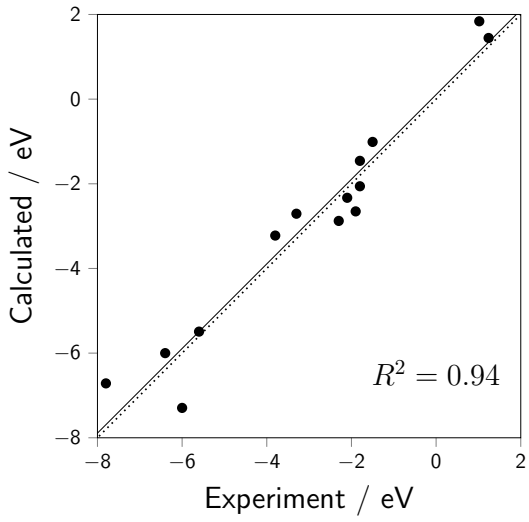


Graphical abstract.